Sensor fault/failure correction and missing sensor replacement for enhanced real-time gas turbine diagnostics

Amare Fentaye[1], Valentina Zaccaria[2], and Konstantinos Kyprianidis[3]

[1,2,3]*Future Energy Center, Mälardalen University, 72123 Västerås, Sweden*

amare.desalegn.fentaye@mdu.se
valentina.zaccaria@mdu.se
konstantinos.kyprianidis@mdu.se

ABSTRACT

Gas turbine sensors are prone to bias and drift. They may also become unavailable due to maintenance activities or failure through time. It is, therefore, important to correct faulty signal or replace missing sensors with estimated values for improved diagnostic solutions. Coping with a small number of sensors is the most difficult to achieve since this often leads to underdetermined and indistinguishable diagnostic problems in multiple fault scenarios. On the other hand, installing additional sensors has been a controversial issue from cost and weight perspectives. Gas path locations with difficult conditions to install sensors is also among other sensor installation related challenges. This paper proposes a sensor fault/failure correction and missing sensor replacement method. Auto-regressive integrated moving average models are employed to correct measurements from faulty and failed sensors. To replace additional sensors needed for further diagnostic accuracy improvements, neural network models are devised. The performance of the developed approach is demonstrated by applying to a three-shaft turbofan engine. Test results verify that the method proposed can well-recover measurements from faulty/failed sensors, no matter with small or major failures. It can also compensate key missing temperature and pressure measurements on the gas path based on the data from other available sensors.

Keywords: Gas turbine sensors; sensor fault; sensor failure; signal reconstruction; missing sensor replacement

1. INTRODUCTION

The quality and quantity of performance data collected along the gas path is key for an accurate gas turbine diagnostics. This depends on the number and type of sensors installed in real-life. In principle, gas path sensors should preferably be placed in the entry and exit of the critical gas path components, to get the complete picture of the engine health. However, this is not often possible in real situations for several reasons. The major sensor related challenges from the diagnostic perspective are discussed as follows.

The first challenge is measurement noise. Noise affects early fault detection ability by hiding low-level fault signatures. It also increases false alarms during harsh operating conditions. Additionally, noise is known to cause Smearing effects in physics driven diagnostic methods (A. Fentaye, Zaccaria, & Kyprianidis, 2021; Zaccaria, Fentaye, Stenfelt, & Kyprianidis, 2020). Data denoising prior to fault diagnostic activities (Y. G. Li, 2002; Sadough Vanini, Meskin, & Khorasani, 2014) and developing noise tolerant diagnostic methods (Bettocchi, Pinelli, Spina, & Venturini, 2006) are the two widely studied solutions.

A sensor fault/failure is the second challenge (Jombo, Zhang, Griffiths, & Latimer, 2018). Bias and drift are the two known forms of a sensor fault. Bias is a systematic measurement error which results in fixed and abrupt shifts. Installation errors, high vibrations and harsh working conditions can be the root causes. Drift is the other source of inaccurate measurements associated with sensor age. In some catastrophic working environments, a complete sensor failure is also expected. This includes not receiving signals and stuck to some specific readings. To diagnose an engine with a sensor fault/failure occurrence, either the faulty signals should be corrected first, or the diagnostic system should be tolerant enough to the corrupted data (J. Li & Ying, 2020; Lu, Li, Huang, & Jia, 2020). Another alternative is separating sensor faults from component faults before conducting any further fault analysis (Ogaji & Singh, 2003).

The third challenge is that certain sensors may become unavailable through time due to maintenance activities or hostile operating conditions. This will lead to fleet engines having different gas path sensors, particularly between the older engines and brand-new ones. Consequently, a life-cycle

performance monitoring and diagnostic system needs to be modified to cope with the available sensors, or the missing sensor must be installed or automatically replaced by estimated values from the remaining measurements. Modifying the performance monitoring and diagnostic system to cope with the remaining sensors may be difficult, since this may cause undistinguishable failure modes, underdetermined diagnostic problem, or may have a significant impact on the diagnostic accuracy. The second alternative is to automatically replace the missing sensor by estimated values from redundant and other available measurements. The estimation can be performed based on physics (Aivaliotis, Georgoulias, Arkouli, & Makris, 2019; X. Zhou, Lu, & Huang, 2019) as well as using machine learning methods (Kramer, 1992).

Sensors can also be missing due to absence of technology. For instance, high-pressure turbine (HPT) entry and exit temperature and pressure sensors are unavailable due to the high gas temperature. Nevertheless, these measurements are vital to discriminate failure modes between the gas turbine hot components (A. Fentaye, Zaccaria, Rahman, Stenfelt, & Kyprianidis, 2020; Zaccaria et al., 2020; X. Zhou et al., 2019). It is technically possible to measure HPT and intermediate-pressure turbine (IPT) blade metal temperatures using a pyrometer. For instance, the RB199 and EJ200 military turbofan engines have a pyrometer on the HPT. But this is not available yet for civil aeroengines and does not represent the actual gas path temperature either.

Cost and weight reduction is another reason why some configurations do not include some measurements. Historically, gas turbine sensors are installed primarily for safety and control purposes. Mostly they are equipped with less than 100 sensors. Modern gas turbines, in contrast, are equipped with over 5000 sensors in total. (Afman, Prasad, & Antolovich, 2017) This includes additional gas path temperature and pressure probes installed for diagnostic reasons. However, several studies on gas turbine diagnostics such as (Ganguli, 2002; Jasmani, Li, & Ariffin, 2011; Simon & Rinehart, 2016) indicated that even the modern gas turbines are still missing some useful gas path measurements which could potentially improve the diagnostic accuracy considerably. A measurement selection study conducted for the Rolls-Royce RB211-24G showed that the high-pressure compressor (HPC) exit temperature (T5), HPT exit pressure (P9), and power turbine (PT) exit temperature (T12) measurements are among the most critical measurements to accurately diagnose the engine gas path (Jasmani et al., 2011). However, all these sensors are not included in the installation. Hence, due to the trade-off between cost plus weight reduction and improving diagnostic accuracy, the decision of installing more sensors is controversial.

Redundancy between measurements (Jasmani et al., 2011) and singularity (Kaboukos, Oikonomou, Stamatis, & Mathioudakis, 2003) are additional challenges of sensors for fault diagnostics. Since sensors are basically installed for the sake of control and safety, some of them may not be useful for diagnostics due to redundancy and singularity issues. Redundancy of measurements is the phenomenon of having two or more sensors with high correlation, while singularity is the state of sensors not responding to performance changes.

Lack of sufficient measurements due to the above highlighted reasons highly affects the maintenance decision making process. For model-based diagnostic approaches, the common way to deal with underdetermined and undistinguishable problems is to choose the best subset of the performance parameters that substantially represent the engine condition (Kaboukos et al., 2003). However, this technique is not effective enough since changes from the removed performance parameters propagate to the selected ones (Simon & Garg, 2009). Two measures can be taken to overcome the shortcoming: installing additional sensors or replacing the missing sensors with estimates. The former had not been of interest to both engine manufacturers and end users due to sensor related costs. Using models as virtual sensors has become indispensable in modern industry for process control, online monitoring, and diagnostics (Jiang, Yin, Dong, & Kaynak, 2021; Kamat & Madhavan, 2016). Recently, this topic has been also receiving attention by the gas turbine community (Afman et al., 2017; J. Zhou, Liu, & Zhang, 2016).

This paper aims to explore the use of autoregressive integrated moving average (ARIMA) models to correct measurements from faulty sensors as well as failed sensors until recalibration or reinstallation is performed. Two modes of operation are considered: when a sensor fault/failure occurs while the engine is under the normal degradation mode and when a sensor fault/failure simultaneously occurs with a component fault. Neural network (NN) models are employed to replace missing sensors due to maintenance activities and additional sensors required to improve diagnostic accuracy.

The rest of the paper is organized as follows. Section 2 describes the method proposed and the case studies used to demonstrate and validate the method. The implementation results to a test case aeroengine with detailed discussion is presented in Section 3, followed by key concluding remarks.

2. METHOD

A generic framework shown in Figure 1 is proposed to address the above discussed sensor problems. From the diagnostic perspective, the first step is selecting the best measurement set that can allow accurate gas path analysis (GPA). Measurements are selected through a sensitivity and correlation analysis. Even among those limited measurements, few of them should be removed, if they are highly correlated with other measurements and/or insensitive to key performance deviations. Various combinations of measurements can also be needed depending on power setting parameters and flight conditions considered.

One of the widely applied methods to deal with limited sensors is choosing the subset providing maximum accuracy. For an invertible system matrix, the number of performance parameters should be reduced to the number of measurements selected. Checking all the possible performance parameter combinations and selecting the subset with maximum accuracy is an iterative process. This approach is prone to error propagation problem due to the unestimated performance parameters and time consuming. Observability analysis can help reduce some of the performance parameters showing high correlation. All the remaining gas path faults should be easily isolable by interpreting the measurement deviations. Choosing among the highly correlated performance parameters to be discarded could be decided based on user's priorities (Stenfelt & Kyprianidis, 2022).

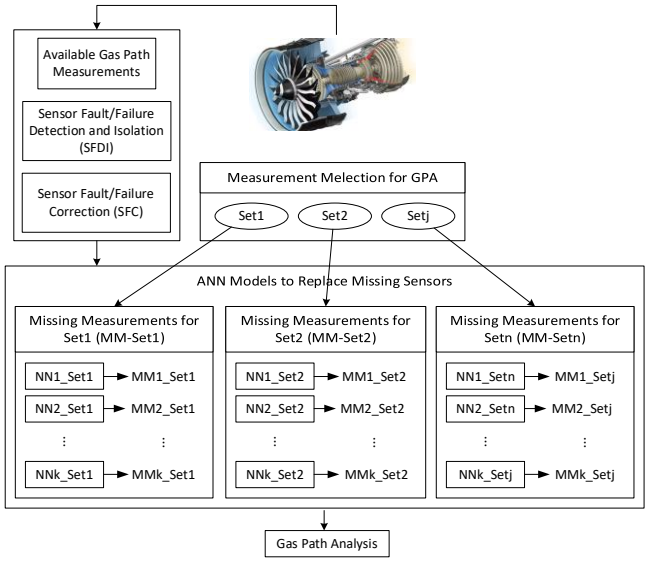

Figure 1. Proposed framework.

In this proposed framework, Figure 1, a full set of health parameters associated with critical gas path components were considered. The necessary measurements were selected through a sensitivity and correlation analysis using performance model of the engine. Unavailable physical measurements are replaced by independently acting NN models developed based on the available information. One important point to note here is that, unlike for diagnostics, if two or more measurements among the available ones are showing high correlation, none of them should be discarded. They are important for each other's predictions during failure.

Since some sensors could become unavailable through time due to maintenance events and hostile operating conditions, the physical sensors available could vary with the engine age. This decreases the number of input measurements to the NN models, while increasing the number of NN modules required to replace missing sensors. Suppose the engine is equipped with m sensors when it was brand new and n measurements are selected for accurate invertible diagnostics, m-n NN modules will be needed to replace the missing sensors. To account missing sensors through time, the NN method should be evaluated for fewer instrumentation suites as well.

In addition to missing sensor cases, a sensor can start providing false readings (due to bias or drift faults) or fixed readings (due to a complete failure) as illustrated in Figure 2. To continue the plant operation, process monitoring, and diagnostic tasks with no interruption, those readings should be automatically replaced by estimated values. In this paper, a forecasting approach was applied to recover inaccurate signals due to a sensor fault/failure. Actual measurements after the detection point are estimated based on the principle of time-series forecasting, by projecting the values before the sensor fault/failure has been detected. The popular forecasting method, ARIMA, is used. However, in a complete engine health monitoring system, this step should be preceded by a sensor fault detection and isolation (SFDI) process, which is not the scope of this paper.

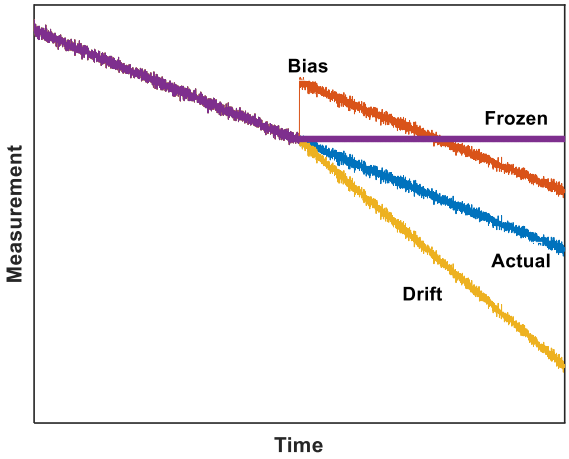

Figure 2. Schematic illustration of a sensor fault/failure in a deteriorating engine.

2.1. Sensor Fault/Failure Correction using ARIMA

The Box-Jenkins ARIMA is a statistical technique widely used for time-series forecasting. It is often designated as ARIMA(p,d,q). and consists of three key parameters: Autoregression (AR), Integrated (I) and Moving Average (MA). The AR part fits a time-series data and forecast future values based on previous values. The MA term uses past errors to make future predictions. The "I" term is needed to make the time-series stationary by taking differences, with d order of transformation. The underling mathematics can be expressed as

$$y_t = \alpha + \gamma_1 y_{t-1} + \gamma_2 y_{t-2} + \cdots + \gamma_p y_{t-p} + \varepsilon_t + \beta_1 \varepsilon_{t-1} + \beta_2 \varepsilon_{t-2} + \cdots + \beta_q \varepsilon_{t-q} \quad (1)$$

where y_t is the actual value at time t and ε_t is the associated normally distributed random error, α and γ represent model parameters, p and q are integer values that indicate orders of

the AR and MA models, respectively. q=0 ⇒ AR model of order p, and p=0 ⇒ MA model of order q.

Four main steps are required to develop an ARIMA model: model identification, parameter estimation, model validation, and forecasting. The first step is used to determine the p, d, and q values from the sample data. It also involves converting the series to stationary through differencing. In the second step, α and γ are computed to optimize the overall error between the predicted and actual input-output data. Least-squares method or other nonlinear optimization techniques can be applied here. Once these two steps are completed, the accuracy of the ARIMA model is verified using new data. The forecasting step is then followed for future timesteps.

ARIMA models have been widely used for engine RUL forecasting so far (Marinai, Singh, Curnock, & Probert, 2003). In our proposed framework, ARIMA is used to reconstruct measurement errors induced by a sensor fault or failure. This is important to avoid unnecessary downtimes for sensor maintenance. Particularly, if the problematic sensor is in the control loop, the reconstructed values can automatically be used for that period to continue the system process without any interruption plus estimate the magnitude of the engine deterioration. Regardless of knowing the type of sensor problem and its magnitude, the ARIMA model forecasts the actual readings based on the readings collected before the problem has been detected. Using the available fault-free signals from the same sensor and correcting the error part through forecasting is more effective than estimating the values based on measurements from other fault free sensors.

However, if a sensor bias is detected due to installation errors, the ARIMA model cannot be applied. Instead, the signals from this sensor should be replaced by a NN model estimates until a reinstallation or recalibration measure is taken. Moreover, if a component fault occurs after a sensor failure, the failed sensor readings should be replaced with estimated values from the NN module. Because the component fault induced measurements cannot be predicted by the ARIMA model based on the normal data or trend before the sensor failure.

2.2. Missing Sensor Replacement using NNs

The typical feed-forward multilayer perceptron has a proven performance record to learn relationships between variables from data and make accurate predictions. In the method proposed, independently acting NN models are developed for each sensor as a regression problem to replace when they are missing, and to replace other additional sensors required for enhanced diagnostic solutions. All available measurements were used as input to each network. The output is the estimated version of a weighted sum of the input.

Model hyperparameters for each NN estimator were determine through a training process the Levenberg-Marquardt backpropagation algorithm. Although a NN model with one hidden layer, with sufficient neurons, is known to be capable enough to approximate most nonlinear regression problems, different number of hidden layers (up to 3) and neurons (up to 60) were evaluated. Variety of activation functions (tanh, logsig, and ReLU) and optimization algorithms (Adam, RMSProp, and sgdm) with different data structure and number of epochs were also checked. The most appropriate network structure was then selected based on the training time, accuracy, and robustness. The Adam optimization algorithm and ReLU activation function showed better performance. The accuracy of the predictions was assessed using the standard deviation (σ) mean absolute error (MAE) and root mean square error (RMSE) indicators.

2.3. Case study: three-shaft turbofan engines

The schematic of the case study engine is shown in Figure 3. Full set of performance parameters, i.e., efficiency and flow capacity for the Fan, intermediate-pressure compressor (IPC), HPC, HPT, intermediate-pressure turbine (IPT), and low-pressure turbine (LPT) were considered. Table 1 presents selected measurements via an observability analysis using the engine performance model and the measurement noise considered. The noise incorporated was a normally distributed Gaussian noise with zero-mean and standard deviation varies as percentage of the actual sensed values.

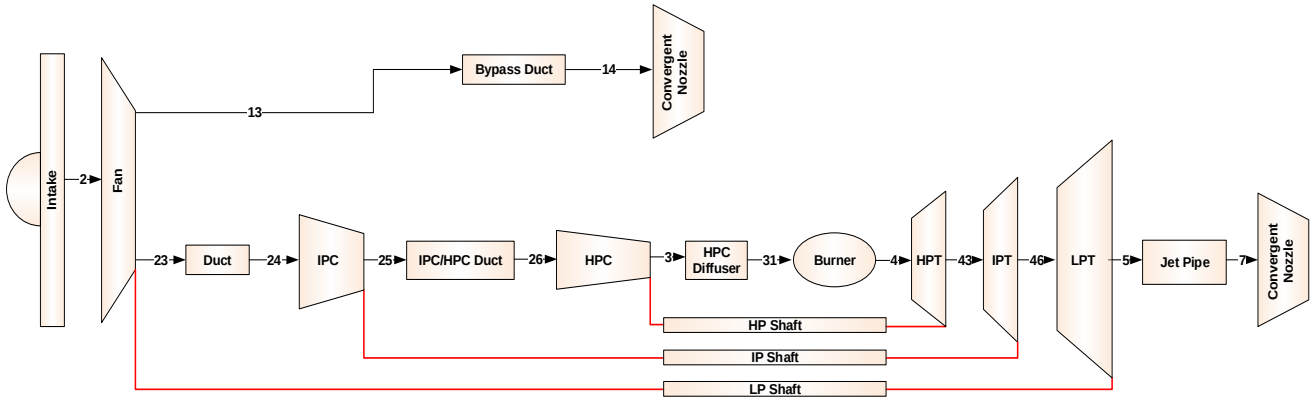

Figure 3. Schematics of three-shaft turbofan engine with measurement locations.

Table 1. Selected measurements for 3-shaft turbofan engine.

Measurement parameter	Notation	Unit	Noise (σ)
IPC inlet total temperature	T23	K	±0.4%
IPC inlet total pressure	P23	kPa	±0.25%
IPC exit total temperature	T25	K	±0.4%
IPC exit total pressure	P25	kPa	±0.25%
HPC exit total temperature	T3	K	±0.4%
HPC exit total pressure	P3	kPa	±0.25%
HP shaft speed	N4	rpm	±0.05%
IP shaft speed	N43	rpm	±0.05%
LP shaft speed	N46	rpm	±0.05%
HPT exit total pressure	P43	kPa	±0.25%
IPT exit total pressure	P46	kPa	±0.25%
LPT exit total temperature	T5	kPa	±0.25%

Based on (Marinai, 2004; Saias, Pellegrini, Brown, & Pachidis, 2021), N4, N44, N46, T25, P25, T3, P3, T46, and T5 are considered mostly available sensors for the commercial 3-shaft turbofan engine. However, sensitivity and correlation analysis results indicate that, N4, N44, N46, T23, P23, T25, P25, T3, P3, P43, P46, and T5 are important to distinguish and estimate the full set of health parameters of the turbofan gas path. Although sensors that have strong correlation between them are not needed in the main diagnostic scheme, they are useful to estimate each other when they fail. That is why high correlation sensors are included in the proposed method. To address the sensor fault/failure correction and missing sensor replacement problems, the following cases were investigated:

1. A single sensor fault/failure was considered and independently acting ARIMA models devised for each available sensor for correction. The engine was under gradual degradation mode.
2. Sensor fault/failure correction was carried out when it simultaneously occurs with a component fault. It is less likely to occur both a sensor fault/failure and a component fault together, but for the sake of inclusiveness this case was also investigated.
3. Four independent NN modules were devised to replace the missing T23, P23, P43, and P46 measurements.
4. Six other NN estimators were developed for the available measurements T25, P25, T3, P3, T46 and T5 to replace them when they are missing.
5. The sensitivity of T23, P23, P43, and P46 estimators was also analysed when case 4 happens.

Data required for training and testing was generated via model simulation. In-house software EVA was used for the simulation as described in (Kyprianidis, 2017). A database of 127080 random inputs was generated considering healthy, deteriorated, and faulty engine conditions. For the sake of generic estimation models, the fault patterns were derived from 63 single and multiple fault types, obtained by considering all possible combinations of the six gas path components taken *r* each time (where r = 1, 2, …, 6). The fault magnitude (FM) was a function of efficiency and flow capacity changes (ΔΓ:Δη) as expressed in Equation (2). For the Fan and the two compressors, equal fault magnitudes (up to 5%) were considered. To accommodate possible ratio differences between efficiency and flow capacity performance factors (A. D. Fentaye, Baheta, Gilani, & Kyprianidis, 2019), 12 different ratios (from 1:1 to 4:1) were considered. Likewise, for the three turbines, equal fault magnitudes (up to 4%) with similar ΔΓ:Δη ratios, ranging from 1:3 to 3:1, were considered.

$$FM = -\Delta\eta\sqrt{1+\left(\Delta\Gamma:\Delta\eta\right)^2} \tag{2}$$

The 127080 dataset was divided in to three groups: 70% for training, 15% for validation and 15% for test. For further testing the generalization performance of the estimators, a different set was generated from bleed valve leakage faults. Up to 7% leakage faults were considered for each compressor to generate 140 sample points in total. This dataset is referred in this paper as a blind test case data.

3. RESULTS AND DISCUSSION

3.1. For the ARIMA model

The first part of the proposed method is faulty signal reconstruction using ARIMA. This part aims to correct sensor fault/failure corrupted measurements via the concept of time-series forecasting. When a sensor malfunction is detected, the measurements of that sensor before the malfunction is started are, in principle, considered and the actual values for the affected timesteps are forecasted. However, since a delay in the detection is inevitable, typically for drift fault scenarios, some previous measurements should be discarded. This is because the future timestep predictions are influenced primarily by the current and the closest previous measurements in the time-series.

Two different scenarios were taken into consideration. The first is when a sensor fault/failure occurs while the engine is undergoing through the state of gradual deterioration. The second is when a sensor fault/failure occurs together with a component fault. Gradual deterioration is a natural phenomenon that a gas turbine engine undergoes over its lifetime. This causes slow and simultaneous changes on the gas path measurements with time. Measurement changes are used to track performance trends, but at the same time, a sensor can also fail or become faulty. To be able to track the performance trend of the engine with no interruption, the corrupted data should automatically be corrected.

During training, three different datasets were considered. The first set was used to train the ARIMA model. Unseen dataset was then used to evaluate the performance of the trained model. Once the validation step was completed, the model was used to forecast future timestep values. Figure 4 shows the results obtained for the IPC delivery temperature in

comparison with the original dataset. The x-axis represents timesteps in "flight cycles" and the y-axis the measured values. The first 1500 data points (red line with diamond marks) indicate the training results, the next 500 points (green line with asterisk) show the test results, the following 500 points (blue line with plus sign marks) refer to the forecasted values, and the black label dedicated to the original dataset with no sensor fault/failure effects. It can be seen in Figure 4 that the forecasted values are more accurate and smoother than the measured values. The results from the remaining sensors are not included here due to space limitation.

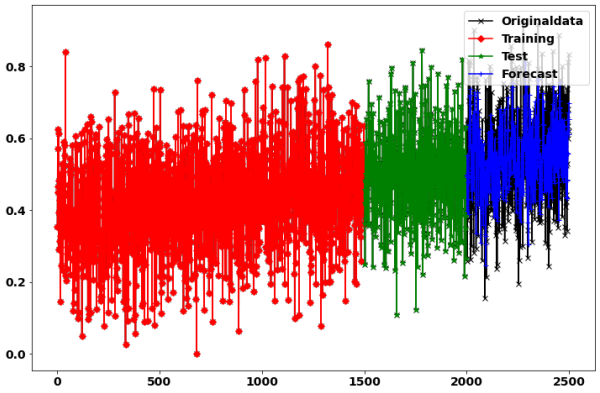

Figure 4. T25 fault/failure correction through forecasting using ARIMA.

In the second problem scenario, a sensor fault/failure occurrence in a faulty engine was analysed. When a component fault occurs, a set of measurements show considerable deviations from the gradual trend. The evolution period of component faults is shorter than the gradual deterioration. If one of the important sensors is failed or become faulty simultaneously with a component fault (although less likely to occur), the ARIMA model will correct the sensor problem. As illustrated in Figure 5, regardless of knowing the type of the sensor malfunction (bias, drift, or complete failure), just based on the detection information, the ARIMA model predicts the actual measurement using the faulty engine data collected before the sensor malfunction is detected. Avoiding the concern to identify the type and magnitude of the sensor malfunction reduces the complexity of the diagnostic problem and computational time. Figure 6 shows training results (red line with diamond marks), test results (green line with asterisk marks) and forecasting results (blue line with plus sign marks) obtained for N4 compared to the original dataset. Similar performances were recorded for the remaining sensors as well, but they are not presented in this paper due to space limitations. The ARIMA model was able to forecast N4 for the 100 future values with 2.13 RMSE. If required, it can also continue forecasting the values after the 100 future flight cycles without losing its accuracy. Moreover, it can be seen in Figure 6 that the forecasted values are smoother than the measured values due to the MA model.

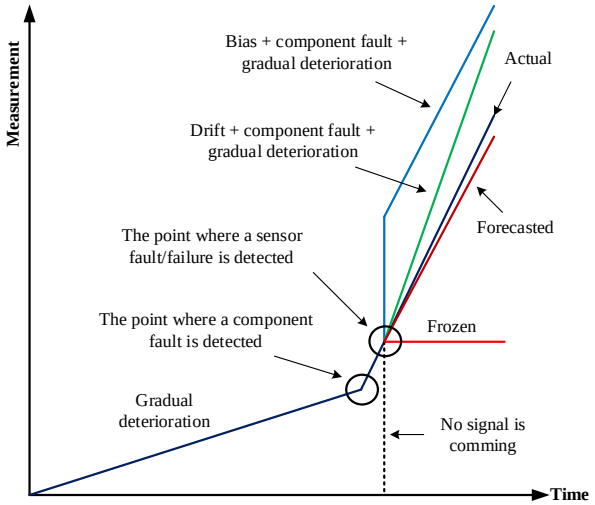

Figure 5. Schematic illustration of a sensor malfunction in a deteriorating faulty engine.

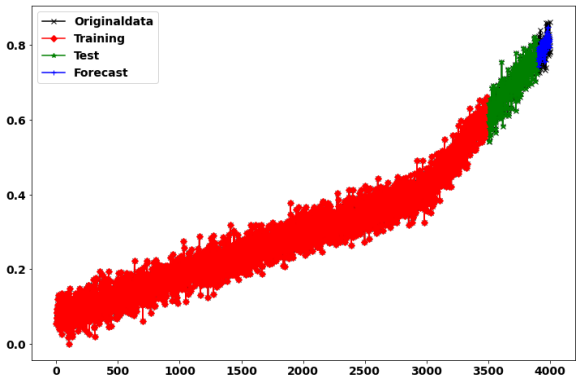

Figure 6. N4 fault/failure correction when a malfunction is detected on N4 in a deteriorating faulty engine.

3.2. For the NN models

Four individual NN models are developed to replace T23, P23, P43, and P46. These four sensors are considered physically unavailable for the turbofan engine. However, they are among the key measurements to distinguish between the Fan, IPC, HPC, HPT, IPT, and LPT faults and accurately estimate their severity. Two different datasets were used to train and verify the NN models. First, the 127080 dataset was randomly divided in to three groups: 70% for training, 15% for cross-validation and the remaining 15% for test. The estimation accuracy of the NN models were examined based on the MAE and σ of the estimation errors in percent. These two parameters are selected to compare the prediction error with that of the Gaussian noise imposed to the data. Figure 7 shows 100 sample normalized test prediction errors. It compares the estimation errors with the measurement noise incorporated. It is seen that the predicted values are smoother and less affected by noise than the measured ones. This is also shown in Table 2 that all estimation error σ values are lower than the associated measurement noise values considered.

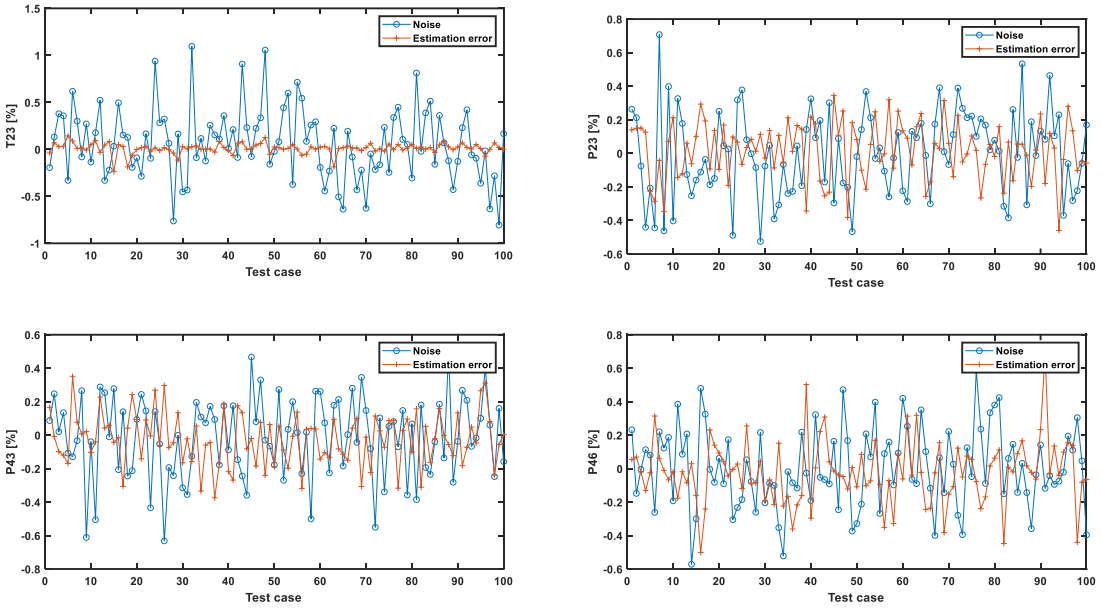

Figure 7. Estimation errors vs. the measurement noise incorporated, 100 random test cases out of the 19,062 test cases.

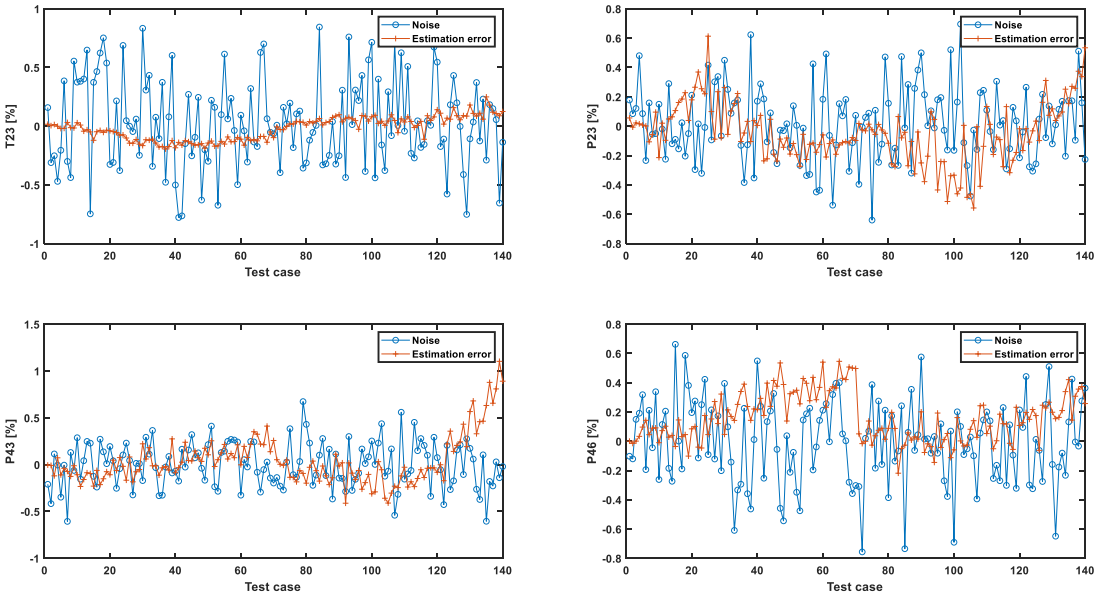

Figure 8. Estimation errors vs. the measurement noise incorporated, for the leakage fault data set.

Table 2. Prediction error vs. measurement noise added.

Error	T23	P23	P43	P46	Reference
Prediction MAE	0.006	-0.002	0.000	-0.001	Measured value
	-0.002	0.003	0.001	0.004	Actual value
Prediction error σ (%)	0.399	0.315	0.297	0.294	Measured value
	0.043	0.189	0.167	0.157	Actual value
Noise σ (%)	0.4	0.25	0.25	0.25	

When applying the blind test data, the results shown in Figure 8 were obtained. The first 70 points represent the estimated measurements associated with the IPC leakage fault and the cases from 71 to 140 are the estimated measurements for the HPC leakage data. To show how far the measurements with leakage faults are from the 127080 training data feature space, the equivalent performance parameter deviations for the Fan, IPC, HPC, HPT, IPT, and LPT were estimated through an adaptive scheme and presented in Figure 9. The equivalent fault magnitude estimated for the Fan, HPT, and IPT reaches up to 8.5%, which is greater than twice of the

fault magnitude considered for the 127080 data. For the HPC, it is approximately 1.6 times and for the IPC and the Fan 1.2 times the fault magnitude used to generate the 127080 set. This proves the generalization capability of the NN estimators developed. Enlarging the training domain could also further improve the estimation accuracy of the models.

The effect of missing one sensor among T25, P25, T3, P3, T46 and T5 on the accuracy of T23, P23, P43, and P46 estimators was also analysed. Figure 10 and Table 3 show test results for the leakage fault data. For all the measurements, estimation errors often fall within the threshold of the measurement noise incorporated. As shown in Figure 10, the error increases with increasing the magnitude of the leakage faults. Particularly, when the effect of the leakage faults on the input measurements excides the equivalent component fault effects. This is expected since the input data distribution starts significantly shifting from the training data space. Although the obtained accuracy is satisfactory, it could also be further improved by increasing the training feature space.

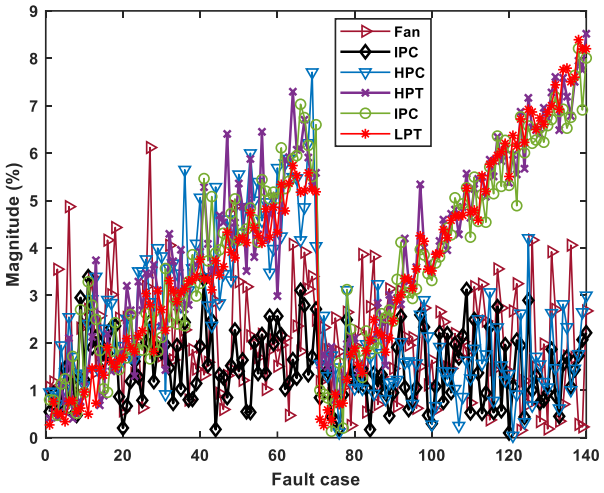

Figure 9. Performance parameter deviations induced by the IPC and HPC leakage faults.

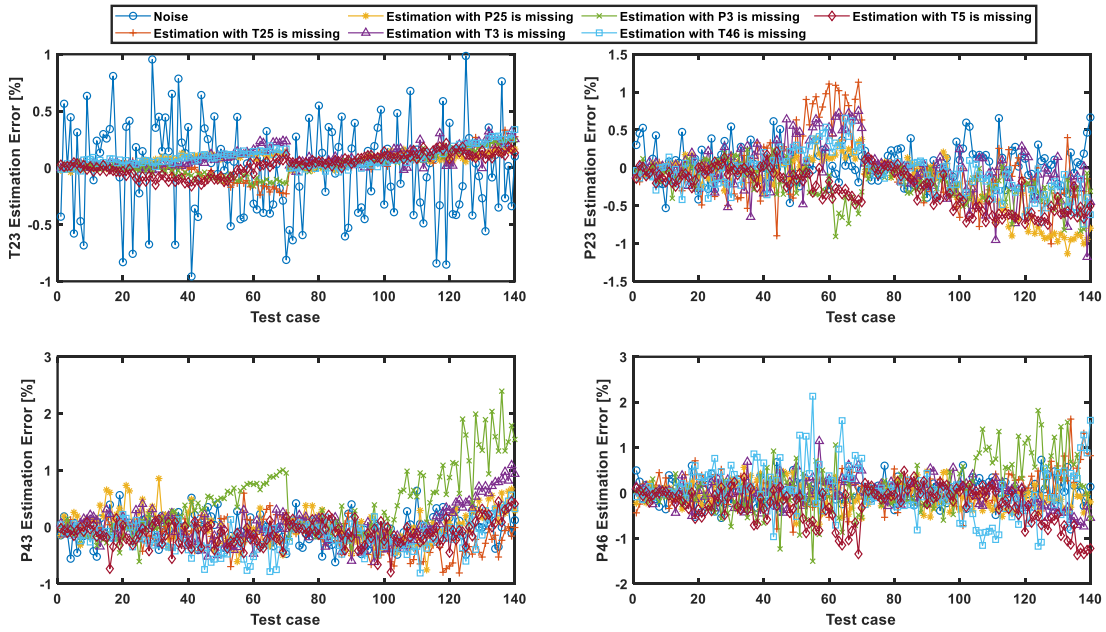

Figure 10. T23, P23, P43, P46 test results for the leakage dataset when one of T25, P25, T3, P3, T46, and T5 is missing.

Table 3. Calculated RMSE values for estimated T23, P23, P43, and P46 measurements when one of the T25, P25, T3, P3, T46 and T5 is missing, for the leakage fault dataset.

Estimated	Missing sensor					
	T25	P25	T3	P3	T46	T5
T23	0.143	0.442	0.594	0.275	0.489	0.441
P23	0.253	0.251	0.398	0.226	0.194	0.427
P43	1.809	2.952	1.332	2.630	1.480	1.941
P46	0.550	1.718	0.581	2.567	1.299	1.506

The capability of the NN models to accurately estimate T25, P25, T3, P3, T46 and T5 when one among them is missing was also investigated. If, for example, T25 is missing, it will be estimated from the remaining measurements: N4, N44, N46, P25, T3, P3, T46, and T5. The standard deviation of the estimation error for each of the six NN modules, for the leakage fault dataset, is presented in Table 4. It is seen in that the estimation error for T25, T46 and T3 is approximately half times the measurement noise considered. The estimation error for T5, on the other hand, is higher, almost twice of the measurement noise incorporated. This is expected because

T5 is shown to have very low correlation with T25, P25, T3, and P3. Similarly, the estimation error for P25 and P3 is higher. The reason could be since P25 and P3 are the most useful measurements to estimate bleed leakages and flow capacity in the two compressors, and since they are also the only pressure measurements available on the gas path, estimating them based only on the other temperature and speed measurements seams relatively difficult. In particular, the estimation error associated with the IPC bleed leakage data was higher than the HPC bleed leakage data for both P25 and P3. For the T25 case, the error for the IPC leakage data was equivalent to a soft sensor fault. Whereas for the HPC leakage data, the error was close to the measurement noise added. Including some leakage induced measurements in the training data sample may improve the accuracy of the two pressure estimators.

Table 4. T25, P25, T3, P3, T46 and T5 estimation accuracy for the leakage fault data set vs. measurement noise added.

Error σ	Estimated measurement					
(%)	T25	P25	T3	P3	T46	T5
Estimation	0.245	1.000	0.199	0.983	0.256	0.777
Noise	0.400	0.250	0.400	0.250	0.400	0.400

4. CONCLUSION

A sensor fault/failure correction and missing sensor replacement method is proposed for three-shaft turbofan engines. In this method, Autoregressive integrated moving average and feedforward neural networks are utilized. The former is responsible to correct faulty measurements through time-series forecasting. A set of neural network models are also devised to replace important sensors for diagnostics which are not installed from the beginning or missed through time due to maintenance activities and damages. When the engine is brand new equipped with full instrumentation suite, the neural network models are used to replace additional measurements required for more advanced diagnostic solutions. Another set of neural network models is developed to replace missing sensors sometime in the engine life cycle. This kind of sensor fault/failure correction and missing sensor replacement system is important in real-time to enable a continuous engine monitoring and diagnostic process with no interruption for re-calibration and re-installation. Additionally, the missing measurement may result in underdetermined problem, indistinguishable failure modes, and inaccurate severity level estimation results.

Performance data generated from the turbofan engine model under different degradation scenarios were used to train and evaluate the method proposed. For all scenarios considered, the faulty sensor signals were able to be corrected successfully with reconstruction errors lower than the measurement noise incorporated. Similarly, for most of the neural network estimators developed, the standard deviation of the test errors was lower than the measurement noise standard deviation considered. The method proposed is flexible for modification to accommodate different engine configurations. However, future work should assess the impact of the sensor scheme on the engine gas path analysis. Ambient condition and operating condition variations were not also included in this paper. Moreover, a linear gradual deterioration profile was considered while gas turbines exhibit nonlinear behavior.

ACKNOWLEDGEMENT

This research was funded by the Swedish Knowledge Foundation (KKS) under the project PROGNOSIS, Grant Number 20190994.

REFERENCES

Afman, J.-P., Prasad, J. V. R., & Antolovich, S. (2017). Real-Time Virtual Sensing of Component Damage Variables in a Gas Turbine Engine. *ASME 2017 Gas Turbine India Conference*, December 7–8, Bangalore, India, V002T11A002. Doi: 10.1115/GTINDIA2017-4706.

Aivaliotis, P., Georgoulias, K., Arkouli, Z., & Makris, S. (2019). Methodology for enabling digital twin using advanced physics-based modelling in predictive maintenance. *Procedia Cirp*, 81, 417-422. Doi: 10.1016/j.procir.2019.03.072.

Bettocchi, R., Pinelli, M., Spina, P. R., & Venturini, M. (2006). Artificial Intelligence for the Diagnostics of Gas Turbines—Part I: Neural Network Approach. Journal of Engineering for Gas Turbines and Power, 129(3), 711-719. Doi:10.1115/1.2431391.

Fentaye, A., Zaccaria, V., & Kyprianidis, K. (2021). Discrimination of rapid and gradual deterioration for an enhanced gas turbine life-cycle monitoring and diagnostics. International Journal of Prognostics and Health Management, 12(3). Doi: 10.36001/ijphm.2021.v12i3.2962.

Fentaye, A., Zaccaria, V., Rahman, M., Stenfelt, M., & Kyprianidis, K. (2020). Hybrid Model-Based and Data-Driven Diagnostic Algorithm for Gas Turbine Engines. *Proceedings of ASME Turbo Expo 2020 Turbomachinery Technical Conference and Exposition*, September 21–25, 2020, GT2020-14481. Doi: 10.1115/GT2020-14481.

Fentaye, A. D., Baheta, A. T., Gilani, S. I., & Kyprianidis, K. G. (2019). A Review on Gas Turbine Gas-Path Diagnostics: State-of-the-Art Methods, Challenges and Opportunities. Aerospace, 6(7), 83. Doi: 10.3390/aerospace6070083.

Ganguli, R. (2002). Fuzzy logic intelligent system for gas turbine module and system fault isolation. Journal of propulsion and power, 18(2), 440-447. Doi: 10.2514/2.5953.

Jasmani, M. S., Li, Y.-G., & Ariffin, Z. (2011). Measurement Selections for Multicomponent Gas Path Diagnostics Using Analytical Approach and Measurement Subset

Concept. Journal of Engineering for Gas Turbines and Power, 133(11). Doi:10.1115/1.4002348.

Jiang, Y., Yin, S., Dong, J., & Kaynak, O. (2021). A Review on Soft Sensors for Monitoring, Control, and Optimization of Industrial Processes. IEEE Sensors Journal, 21(11), 12868-12881. Doi:10.1109/JSEN.2020.3033153.

Jombo, G., Zhang, Y., Griffiths, J. D., & Latimer, T. (2018). Automated Gas Turbine Sensor Fault Diagnostics. Proceedings of ASME Turbo Expo 2018: *Turbomachinery Technical Conference and Exposition*, June 11–15, 2018, Oslo, Norway, GT2018-75229, V006T05A003. Doi: 10.1115/GT2018-75229.

Kaboukos, P., Oikonomou, P., Stamatis, A., & Mathioudakis, K. (2003). Optimizing diagnostic effectiveness of mixed turbofans by means of adaptive modelling and choice of appropriate monitoring parameters. RTO A VT Symposium on "Ageing Mechanisms and Control: Part B - Monitoring and Management of Gas Turbine Fleets for Extended Lift and Reduced Costs", Manchester, UK, 8-11 October 2001, and published in RTO-MP-079(1).

Kamat, S., & Madhavan, K. P. (2016). Developing ANN based Virtual/Soft Sensors for Industrial Problems. IFAC-PapersOnLine, 49(1), 100-105.Doi:https://doi.org/10.1016/j.ifacol.2016.03.036.

Kramer, M. A. (1992). Autoassociative neural networks. Computers & Chemical Engineering, 16(4), 313-328. Doi:https://doi.org/10.1016/0098-1354(92)80051-A.

Kyprianidis, K. (2017). An Approach to Multi-Disciplinary Aero Engine Conceptual Design. Paper presented at the *International Symposium on Air Breathing Engines*, ISABE 2017, Manchester, United Kingdom, 3-8 September 2017 Paper No. ISABE-2017-22661.

Li, J., & Ying, Y. (2020). Gas turbine gas path diagnosis under transient operating conditions: A steady state performance model based local optimization approach. Applied Thermal Engineering, 170, 115025. Doi:https://doi.org/10.1016/j.applthermaleng.2020.115025.

Li, Y. G. (2002). Performance-analysis-based gas turbine diagnostics: A review. Proceedings of the Institution of Mechanical Engineers, Part A: Journal of Power and Energy, 216(5), 363-377. Doi:10.1243/095765002320877856.

Lu, F., Li, Z., Huang, J., & Jia, M. (2020). Hybrid State Estimation for Aircraft Engine Anomaly Detection and Fault Accommodation. AIAA Journal, 58(4), 1748-1762. Doi: 10.2514/1.J059044.

Marinai, L. (2004). *Gas-path diagnostics and prognostics for aero-engines using fuzzy logic and time series analysis*. Ph.D. Thesis, Cranfield University, Bedford, UK. http://dspace.lib.cranfield.ac.uk/handle/1826/6730.

Marinai, L., Singh, R., Curnock, B., & Probert, D. (2003). Detection and Prediction of the Performance Deterioration of a Turbofan Engine. In: TS-005, International Gas-turbine Congress 2003 Tokyo; November 2–7, 2003.

Ogaji, S. O., & Singh, R. (2003). Advanced engine diagnostics using artificial neural networks. Applied soft computing, 3(3), 259-271. Doi: 10.1016/S1568-4946(03)00038-3

Sadough Vanini, Z. N., Meskin, N., & Khorasani, K. (2014). Multiple-Model Sensor and Components Fault Diagnosis in Gas Turbine Engines Using Autoassociative Neural Networks. Journal of Engineering for Gas Turbines and Power, 136(9). Doi:10.1115/1.4027215.

Saias, C. A., Pellegrini, A., Brown, S., & Pachidis, V. (2021). Three-spool turbofan pass-off test data analysis using an optimization-based diagnostic technique. Proceedings of the Institution of Mechanical Engineers, Part A: Journal of Power and Energy, 235(6), 1577-1591. Doi:10.1177/09576509211002311.

Simon, D. L., & Garg, S. (2009). Optimal Tuner Selection for Kalman Filter-Based Aircraft Engine Performance Estimation. Journal of Engineering for Gas Turbines and Power, 132(3). Doi:10.1115/1.3157096.

Simon, D. L., & Rinehart, A. W. (2016). Sensor Selection for Aircraft Engine Performance Estimation and Gas Path Fault Diagnostics. Journal of Engineering for Gas Turbines and Power, 138(7). Doi:10.1115/1.4032339.

Stenfelt, M., & Kyprianidis, K. (2022). Estimation and Mitigation of Unknown Airplane Installation Effects on GPA Diagnostics. Machines, 10(1), 36. Retrieved from https://www.mdpi.com/2075-1702/10/1/36.

Zaccaria, V., Fentaye, A. D., Stenfelt, M., & Kyprianidis, K. G. (2020). Probabilistic model for aero-engines fleet condition monitoring. Aerospace, 7(6), 66. Doi: 10.3390/aerospace7060066.

Zhou, J., Liu, Y., & Zhang, T. (2016). Analytical Redundancy Design for Aeroengine Sensor Fault Diagnostics Based on SROS-ELM. Mathematical Problems in Engineering, 2016, 8153282. doi:10.1155/2016/8153282.

Zhou, X., Lu, F., & Huang, J. (2019). Fault diagnosis based on measurement reconstruction of HPT exit pressure for turbofan engine. Chinese Journal of Aeronautics, 32(5), 1156-1170. Doi:https://doi.org/10.1016/j.cja.2019.03.032.